Journal of Magnetic Resonance 200 (2009) 109–118

Contents lists available at ScienceDirect

Journal of Magnetic Resonance

journal homepage: www.elsevier.com/locate/jmr

Measurement of one and two bond N–C couplings in large proteins by TROSY-based *J*-modulation experiments

Yizhou Liu, James H. Prestegard *

Complex Carbohydrate Research Center, The University of Georgia, Athens, GA 30602, USA

ARTICLE INFO

Article history:
Received 14 April 2009
Revised 18 May 2009
Available online 17 June 2009

Keywords:
RDC
Bicelle
Myristoylated protein
Scalar coupling
J-modulation
TROSY

ABSTRACT

Residual dipolar couplings (RDCs) between NC′ and NC$^{\alpha}$ atoms in polypeptide backbones of proteins contain information on the orientation of bond vectors that is complementary to that contained in NH RDCs. The $^{1}J_{NC^{\alpha}}$ and $^{2}J_{NC^{\alpha}}$ scalar couplings between these atoms also display a Karplus relation with the backbone torsion angles and report on secondary structure. However, these N–C couplings tend to be small and they are frequently unresolvable in frequency domain spectra having the broad lines characteristic of large proteins. Here a TROSY-based *J*-modulated approach for the measurement of small ^{15}N–^{13}C couplings in large proteins is described. The cross-correlation interference effects inherent in TROSY methods improve resolution and signal to noise ratios for large proteins, and the use of *J*-modulation to encode couplings eliminates the need to remove frequency distortions from overlapping peaks during data analysis. The utility of the method is demonstrated by measurement of $^{1}J_{NC'}$, $^{1}J_{NC^{\alpha}}$, and $^{2}J_{NC^{\alpha}}$ scalar couplings and $^{1}D_{NC'}$ and $^{1}D_{NC^{\alpha}}$ residual dipolar couplings for the myristoylated yeast ARF1·GTPγs protein bound to small lipid bicelles, a system with an effective molecule weight of ~70 kDa.

© 2009 Elsevier Inc. All rights reserved.

1. Introduction

Couplings between pairs of spin ½ nuclei are a rich source of information for the structural characterization of proteins. The most common applications involve the use of three bond scalar couplings to restrict torsional angles about the central bond, such as the use of ^{3}J between an amide proton and a H$^{\alpha}$ proton to restrict the ϕ angle between C$^{\alpha}$ and its directly bonded nitrogen [1–4], and the use of residual dipolar couplings (RDCs) to restrict orientations of bond vectors between pairs of spin ½ nuclei, such as that between an amide proton and an amide nitrogen of a ^{15}N labeled protein [5–8]. Interestingly the $^{1}J_{NC^{\alpha}}$ and $^{2}J_{NC^{\alpha}}$ scalar couplings are similar to three bond scalar couplings in their dependence on backbone dihedral angles, but depend on Ψ_i and Ψ_{i-1}, respectively, instead of ϕ [9–11]. Likewise, ^{15}N–^{13}C RDCs provide complementary information to ^{1}H–^{15}N and other larger RDCs in restricting orientations of backbone structural elements [8,12,13]. The heteronuclear dipolar coupling Hamiltonian and the weak *J*-coupling Hamiltonian actually have the same spin part, so measurements of RDCs and *J* couplings usually utilize the same NMR experiments. While most experiments work well for measurement of the larger couplings, application becomes challenging when couplings are small compared to the spectral line widths. This is particularly an issue for ^{15}N–^{13}C couplings in larger proteins. Here we present a set of experiments that prove to be of particular value in these situations.

There has, of course, been considerable work devoted to the design of experiments for the measurement of scalar and dipolar couplings. In the most straightforward applications the couplings are measured from the frequency separations of lines in multiplet structures. The amide ^{15}N–^{1}H *J* coupling of ~93 Hz is usually larger than the ^{15}N/^{1}H line widths of proteins studied by solution NMR and can be determined at relatively high accuracy. The ^{15}N–^{1}H RDCs are manifested as small changes in the doublet splitting and the slight increase in line-width in weakly orientated proteins do not severely degrade the measurement accuracy. The large ^{15}N–^{1}H *J* coupling relative to the ^{15}N transverse relaxation also makes possible the use of an IPAP type experiment, in which the doublet components are separated into different spectra in order to minimize spectral overlap without significant loss of sensitivity [14]. In contrast, the N–C couplings ($^{1}J_{NC'} \approx 15$ Hz, $^{1}J_{NC^{\alpha}} \approx 11$ Hz, $^{2}J_{NC^{\alpha}} \approx 7$ Hz) are small and measurement by frequency separation is usually limited to small proteins where sharp ^{15}N lines are obtainable. The situation can be improved somewhat by allowing the *J* coupling to evolve longer than the chemical shift, thus scaling up the apparent splittings [15–17]. This does not solve the problem of doublet overlap because the line-width is often scaled up proportionally, however, the digitization error is reduced. IPAP type experiments can be used to eliminate overlap of peaks in $^{1}J_{NC'}$ and $^{2}J_{NC^{\alpha}}$ doublets [11] but IPAP is not suitable for the measurement of $^{1}J_{NC^{\alpha}}$ since there is no effective way of selectively creating

* Corresponding author. Fax: +1 706 542 4412.
E-mail address: jpresteg@ccrc.uga.edu (J.H. Prestegard).

1090-7807/$ - see front matter © 2009 Elsevier Inc. All rights reserved.
doi:10.1016/j.jmr.2009.06.010

anti-phase magnetization for N–$C^{\alpha}(i)$ without also creating anti-phase magnetization for N–$C^{\alpha}(i-1)$. The HNCO-based E.COSY type experiments can also be utilized to separate the $^{2}J_{NC^{\alpha}}$ doublets through an extra C′ dimension subject to a much larger $^{1}JC'C^{\alpha}$ coupling [17]. However, due to the absence of a significant $C'(i-1)$–$C^{\alpha}(i)$ coupling, the E.COSY principle is inapplicable to the effective separation of the $^{1}J_{NC^{\alpha}}$ doublets and therefore its measurement is still limited by the ^{15}N linewidth. Another complication associated with small *J*-couplings arises when the RDCs between pairs of atoms become comparable in size to their *J* couplings; this makes RDC sign and size determination ambiguous. In this case, E.COSY style experiments [18] can be employed if one of the weakly coupled spins is coupled to a third spin with a constant of known sign. The sign and size of an RDC can also be determined through variable angle sample spinning that scales anisotropic couplings but keeps scalar couplings unchanged [19].

As an alternative to frequency-based methods, *J* couplings can be obtained by intensity-based methods, including quantitative *J*-correlation [4,22] and *J*-modulation [10,20,21,24] experiments. The main difference between the two is that in the *J*-correlation method, the coupling is obtained from the ratio of two distinct functions correlated by *J*-coupling after a fixed through-coupling transfer period, while in the *J*-modulation method, only a single *J*-modulated function is recorded but at multiple transfer times. Because of its simplicity, the *J*-correlation method is widely used in 3D based experiments. *J*-modulation is more often used in 2D based experiments where a large number of modulation time points can be taken within a reasonable amount of spectrometer time. Because the coupling of interest is usually over-determined, the *J*-modulation experiment offers higher precision [21]. It also has the advantage that errors in derived couplings can be easily estimated based on the quality of multiple-point fitting. The intensity-based methods are applicable as long as chemical shift differences are larger than line widths, regardless of the size of couplings. Thus, they are widely used for the measurement of small homo- and heteronuclear couplings [10,20,22,23]. However, since longer modulation delays are necessary in order to measure small couplings, sensitivity loss from transverse relaxation degrades the performance. This is particularly a problem for large proteins and actually produces a similar problem to that encountered in frequency domain experiments when line widths approach the size of couplings to be measured.

The destructive interference between ^{1}H–^{15}N dipolar interaction and ^{15}N CSA can significantly improve spectral resolution and enhance sensitivity for experiments involving long ^{15}N transverse relaxation periods [25,26]. However, it is difficult to exclusively utilize the ^{15}N TROSY component during the measurement of NH couplings. For example, in frequency separated experiments, at least one of the lines in the multiplet structure is contaminated by the fast anti-TROSY relaxation [14,27,28], while in *J*-modulated experiments, it is hard to avoid a proton π pulse that exchanges TROSY and anti-TROSY magnetizations [21]. In contrast, for the measurement of N–C couplings, the slow ^{15}N TROSY relaxation can be utilized during the entire *J*-modulation delay; this allows the use of the long delay times needed for accurate measurement.

The experimental scheme presented here is directed at the measurement of small ^{15}N–^{13}C couplings in large proteins. The sequence is basically a constant/semi-constant time ^{1}H–^{15}N TROSY experiment [29] with an ^{15}N evolution period modified to allow modulation by selected ^{13}C couplings for various periods of time. The sensitivity is further enhanced by sharing ^{15}N chemical shift evolution with the *J*-modulation periods. For the initial time points where the *J*-modulation periods are shorter than the time required for ^{15}N chemical shift evolution, a semi-constant time evolution is automatically adapted. We also choose to collect a reference spectrum for every modulation delay, in which *J* couplings are refocused so that spectral intensity is only modulated by relaxation. The peak intensity ratio between the *J*-modulation spectrum and the reference spectrum eliminates the contribution from relaxation. The latter approach introduces characteristics of both *J*-correlated and *J*-modulated methods in that a reference function is employed to cancel the relaxation effects and multiple delays are used for non-linear fitting. In addition it eliminates complications due to line widths varying with *J*-modulation periods in the semi-constant time version, it improves fitting accuracy by removing the relaxation rate as a floating parameter, and it allows more flexibility in combining data from different experiments as may occur with unstable samples.

The procedure is illustrated with data on a GDP/GTP switch protein that is involved in vesicle trafficking, namely yARF1·GTP [30]. ARF1 is a 21 kDa member of the RAS super family. It is N-terminal myristoylated, and exposure of this myristoyl chain, in addition to an N-terminal amphipathic helix, is believed to modulate membrane association. We recently reported the solution structure for the GDP bound form of myristoylated yARF1 [31]. Here a bicelle associated GTPγs bound form of the myristoylated protein is used. The effective molecular weight of the complex is estimated to be 70 kDa, a large system that poses a good test for the pulse sequence.

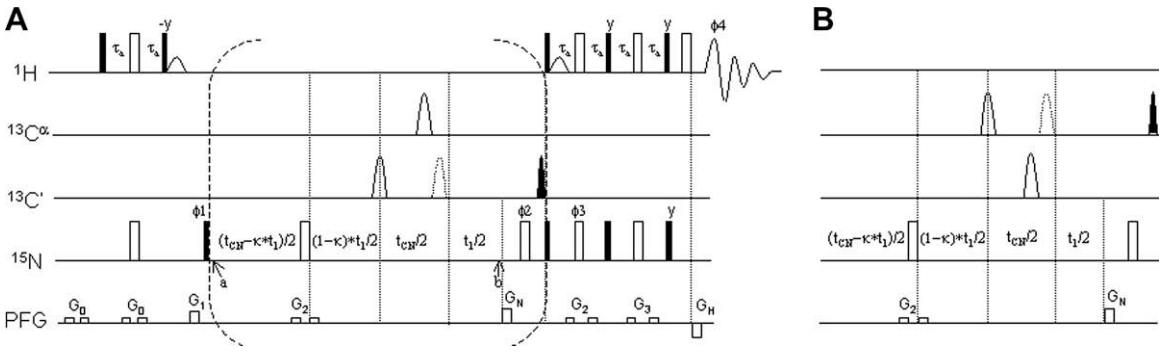

Fig. 1. Pulse sequences for the measurement of $^{1}J_{NC'}$, $^{1}J_{NC^{\alpha}}$, and $^{2}J_{NC^{\alpha}}$ couplings. (A) The sequence for measurement of $^{1}J_{NC'}$. (B) The sequence to replace the part inside the dashed bracket of (A) to allow simultaneous measurement of $^{1}J_{NC^{\alpha}}$, and $^{2}J_{NC^{\alpha}}$ couplings. Narrow solid and wide open bars represent 90° and 180° rf pulses, respectively. The pulses are *x* phased unless otherwise indicated. The scale factor κ is set to 1 if t_{CN} is longer than the maximal t_1 acquisition time $t_{1,max}$, otherwise it is set to $t_{CN}/t_{1,max}$. The C′ 180° and 90° sinc pulses are centered at 174 ppm with a null point at 56 ppm. The C^{α} 180° and 90° reburp pulses are centered at 56 ppm covering a band width of 50 ppm. The sinc water flip-back pulse has a duration of 946 μs. The delay τ_a is $0.91/(4J_{NH}) \approx 2.45$ ms. The phase cycling is: $\phi_1 = \{x, -x\}$, $\phi_2 = \{2(x), 2(-x)\}$, $\phi_3 = \{x\}$ and $\phi_4 = \{-x, x\}$. The gradient G_H and the phase of ϕ_3 are inverted along with the echo/anti-echo acquisition. The *z* gradients are: $G_0 = 1.8G$/cm, 0.5 ms; $G_1 = 26.6G$/cm, 1 ms; $G_2 = 3.6G$/cm, 0.5 ms; $G_3 = 5.4G$/cm, 0.5 ms; $G_N = 31.9G$/cm, 2 ms; $G_H = 32.3G$/cm, 0.2 ms.

Download English Version:

https://daneshyari.com/en/article/5406873

Download Persian Version:

https://daneshyari.com/article/5406873

Daneshyari.com